A Flexible, Micro-Lens-Coupled LED Stimulator for Optical Neuromodulation

Xiaopeng Bi, Tian Xie, Bin Fan, Wasif Khan, Yue Guo, and Wen Li, *Senior Member, IEEE*

***Abstract*—Optogenetics is a fast growing neuromodulation method, which can remotely manipulate the specific activities of genetically-targeted neural cells and associated biological behaviors with millisecond temporal precision through light illumination. Application of optogenetics in neuroscience studies has created an increased need for the development of light sources and the instruments for light delivery. This paper presents a micro-lens-coupled LED neural stimulator which includes a backside reflector and a frontside microlens for light collection and collimation. The device structure has been optimized using optical simulation and the optimized device is able to increase the volume of excitable tissues by 70.4%. Device prototypes have been fabricated and integrated based on an optimization of the device structure. The measurement results show that the light power increases by 99% at an effective penetration depth of 5 000 μm by the fabricated device under various voltages of 2.4–3.2 V.**

***Index Terms*—Microlens, micro-light-emitting diode, optical neuromodulation, optogenetics.**

I. Introduction

OPTOGENETICS has proven to be a revolutionary approach for dissecting neural circuitry, which utilizes light to excite or inhibit the activity of genetically targeted neurons expressing light-sensitive opsin proteins [1]–[7]. Unlike electrical neuromodulation that suffers from indiscriminate activation of cell components (somas, dendrites, and axons) [8], optogenetic neuromodulation uniquely combines cell type-specific control with millisecond time scale temporal resolution in a fully reversible manner [9]. The cell type-specificity in rodents can be achieved by selecting appropriate promoters, for example, CaMKII α for targeting excitatory neurons, glial fibrillary acidic protein (GFAP) for targeting astrocytes, and ppHcrt promoter for targeting hypocretin neurons [10], [11]. Another important benefit of optogenetics over electrical stimulation is that it produces minimal electrical artifacts and instrumental interferences with electrophysiological recording, thereby allowing simultaneous recording of light-evoked neural activity. For these reasons, optogenetics has become a powerful tool for fundamental research of neuroscience in animal models.

Application of optogenetics in neuroscience studies has inspired the development of light sources and instruments for light delivery. Optical stimulation of neural cells is most commonly accomplished by illuminating target neurons with laser, laser diode, or light-emitting-diode (LED) coupled optical fibers [10], [12], [13]. Although such instruments can provide strong illumination, their spatial resolution is limited, and the tethered optical fibers greatly restrict the natural behavior of freely moving subjects. The employment of micro-LEDs (μ-LEDs) offers a great option as the light source for optogenetics [14]. They are power-efficient, low-cost, and suitable for integration with wireless electronics [15]. Furthermore, arrays of individually addressable μ-LEDs have been developed to accomplish multisite *in-vivo* stimulation [16]–[18]. However, a critical challenge of using LEDs as the light source for optogenetics is their intrinsically low out-coupling efficiency and wide irradiation angles due to the Lambertian emission pattern, which results in a big loss of the radiation. Consequently, LEDs must be driven with high power in order to reach the required light intensity of 1 mW/mm^2 and 7 mW/mm^2 for effective activation of excitatory and inhibitory opsins at the target site, respectively [19]. This, however, is not suitable for wireless operation, and could induce potential thermal interference or damage to tissues due to Joule heating effect. Therefore, an extra optical component that can help collimate the LED light is particularly desired, offering capabilities of optical neurostimulation with reduced input voltage and power consumption. To date, little study has been reported on such collimated LED stimulators for optogenetic applications [20], [21].

To address these needs, we propose an implantable, micro-lens-coupled LED neural stimulator to be applied as the light source for optical neuromodulation. A reflector and a microlens were fabricated and integrated with the μ-LED chip for light collection and collimation, respectively, giving rise to a significantly improved light irradiance at near-normal irradiation angles. Built on our preliminary work which presented the design and fabrication of device prototypes [22], this paper carried out an optimization on the device structure using optical simulation, in order to attain optimal collimation and penetration capabilities of light. The optimized device prototypes were then prepared and the measurement of light power transmitting through rat brain tissue was performed to validate the functionality of devices. Both measurement and simulation results imply that the proposed micro-lens-coupled LED stimulator is a promising option as the light source for optogenetic neuromodulation.

Manuscript received February 15, 2016; revised June 9, 2016; accepted July 18, 2016. Date of publication September 20, 2016; date of current version December 7, 2016. This work was supported by the Electrical, Communications and Cyber Systems Division of the National Science Foundation under Award ECCS-1055269. This paper was recommended by Associate Editor D. Demarchi.

The authors are with the Microtechnology Laboratory, Department of Electrical and Computer Engineering, Michigan State University, East Lansing, MI 48824 USA (e-mail: bixiaope@msu.edu; xietian1@egr.msu.edu; fanbin@msu.edu; khanwasi@msu.edu; guoyue@msu.edu; wenli@egr.msu.edu).

Color versions of one or more of the figures in this paper are available online at http://ieeexplore.ieee.org.

Digital Object Identifier 10.1109/TBCAS.2016.2599406

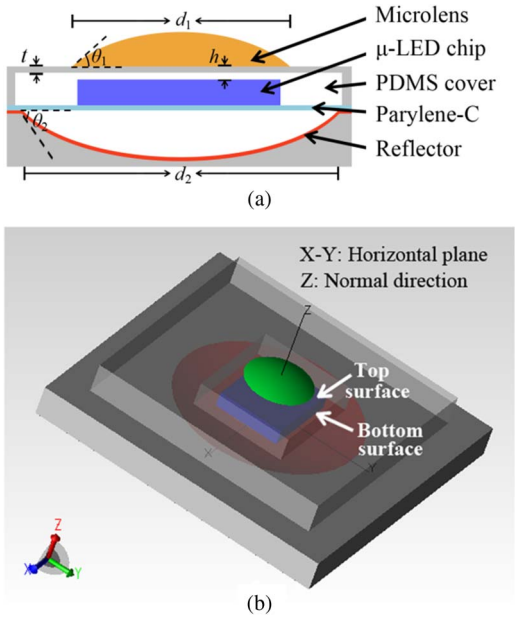

Fig. 1. (a) Structure of micro-lens-coupled LED simulator, which comprises a μ-LED chip, a frontside microlens, and a backside reflector. (b) Structural model of the micro-lens-coupled LED stimulator in the simulation.

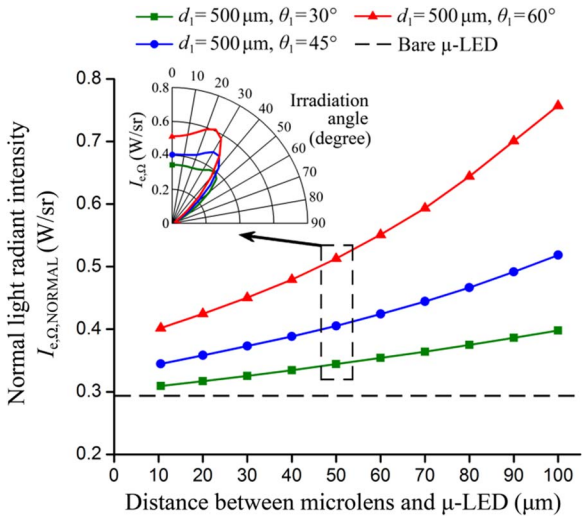

Fig. 2. Simulated normal light radiant intensity $(I_{\mathrm{e},\Omega,\mathrm{NORMAL}})$ for μ-LED-coupled microlenses with a fixed base diameter (d_1) of 500 μm but varied inclined angles (θ_1) of 30°, 45°, and 60°, as a function of the distance between the μ-LED and the microlens (h). The inset shows candela distribution of μ-LED-coupled microlenses that are placed at $h = 50$ μm. The light radiative flux from each side of the μ-LED was set to 1 W. For comparison, the black dash line shows the value of $I_{\mathrm{e},\Omega,\mathrm{NORMAL}}$ for the bare μ-LED.

II. Design, Simulation, and Optimization

A. Design Concept

The proposed micro-lens-coupled LED stimulator comprises three main elements: a μ-LED chip, a microlens, and a reflector, as shown in Fig. 1(a). The μ-LED is placed on a 5-μm-thick Parylene-C substrate, which is biocompatible, flexible, and optically transparent. A polydimethylsiloxane (PDMS) cover is employed to house the μ-LED, and also serves as the substrate in the fabrication of SU-8 microlens. The μ-LED is sandwiched between the microlens and the reflector with center alignment through bonding. Since the unpackaged μ-LED chip used in our experiments radiates light in all directions, the backside reflector is applied to redirect and collect the downward-emitting lights, while the microlens is placed on the frontside of the μ-LED enabling collimation of lights. Surface mounted μ-LED chips (Cree® TR2227TM, 220 μm × 270 μm × 50 μm) with a peak wavelength of 460 nm are used as the light source.

B. Simulation Methods

Optical simulations were performed in Tracepro (Lambda Research Corporation, Littleton, MA) by tracing light rays using the Monte Carlo method to study the properties of the micro-lens-coupled LED stimulator. A typical structural model including all the elements is presented in Fig. 1(b). The surface source property was imported from the irradiation distribution on μ-LED data sheet. Except when specifically mentioned, a light radiative flux of 1 W with a wavelength of 460 nm was set on both the top and the bottom LED surfaces in order to simulate the double-sided illumination. The geometry for each element was drawn based on the design and the optimization of their structures will be discussed later. Candela distribution, which shows the relationship between light radiant intensity $(I_{\mathrm{e},\Omega})$ and irradiation angles, is used to characterize the emission property of the light source. The light radiant intensity is measured in watts per steradian (W/sr). The irradiation angle is defined as the angle with respect to the normal direction to the LED top surface. Especially, the light radiant intensity at 0° on the candela distribution $(I_{\mathrm{e},\Omega,\mathrm{NORMAL}})$ is employed to approximately represent the collimation ability of the light. For a bare μ-LED chip, $I_{\mathrm{e},\Omega,\mathrm{NORMAL}}$ is 0.29 W/sr.

C. Optimization of Microlens Structure

Several parameters have been considered for microlens optimization, including its base diameter (d_1), its inclined angle (θ_1), its distance away from the LED top surface (h), and the thickness of the PDMS layer (t), as shown in Fig. 1(a). It is noteworthy that the PDMS cover is a necessary element in our design because of the following two reasons. First, a fabrication technique called vapor-induced dewetting (VID) [23] is employed to produce SU-8 microlenses directly on the plasma-treated PDMS surface. During the dewetting process, the surface chemistry of PDMS plays a crucial role in determining the range of the inclined angle of microlenses. Second, the lens effect is strongly influenced by the distance between the lens and the μ-LED (h), which can be tuned using PDMS micromolding to achieve the most desired value. On the other hand, in order to minimize the scattering effect while light propagates through PDMS, the thickness of the PDMS cover (t) was kept as small as 10 μm.

Taking the compactness of devices into consideration, d_1 and h were limited to not exceed 600 μm and 100 μm, respectively. The influence of θ_1 on the collimation was first considered. Fig. 2 shows representative curves of $I_{e,\Omega,\mathrm{NORMAL}}$ as a function of h for μ-LED-coupled microlenses with a fixed d_1 of 500 μm but varied θ_1 of 30°, 45°, and 60°. It can be concluded

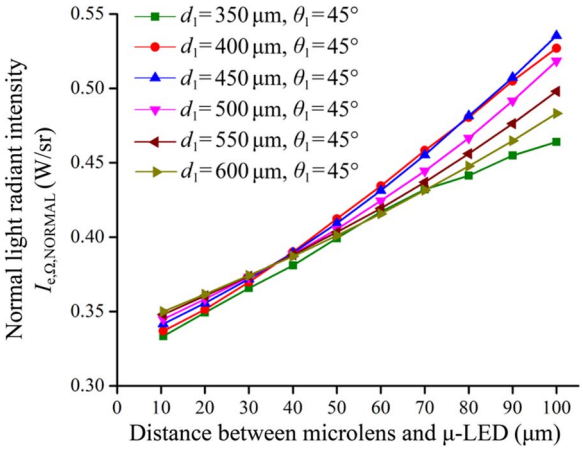

Fig. 3. Simulated normal light radiant intensity ($I_{e,\Omega,\mathrm{NORMAL}}$) for μ-LED-coupled microlenses with a fixed inclined angle (θ_1) of 45° but varied base diameters (d_1) ranging from 350 μm to 600 μm, as a function of the distance between the μ-LED and the microlens (h). The light radiative flux from each side of the μ-LED was set to 1 W.

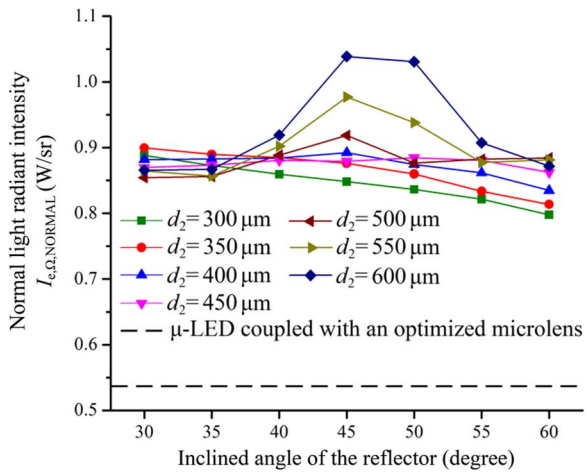

Fig. 4. Simulated normal light radiant intensity ($I_{e,\Omega,\mathrm{NORMAL}}$) for μ-LEDs coupled with an optimized microlens ($d_1 = 450\ \mu$m, $\theta_1 = 45°, t = 100\ \mu$m) and different reflectors with varied diameters (d_2) and inclined angles (θ_2). The light radiative flux from each side of the μ-LED was set to 1 W. For comparison, the black dash line shows the value of $I_{e,\Omega,\mathrm{NORMAL}}$ for the device without a reflector.

that a microlens with a larger inclined angle leads to a stronger light radiant intensity in the normal direction. Such a trend was also observed in our optical simulation for microlenses with varied diameters of 400 μm, 450 μm, 550 μm, and 600 μm. Since our VID process can fabricate microlenses with inclined angles between ~27° to ~47° [23], $\theta_1 = 45°$ is used in the following optimization studies. For microlenses with larger inclined angles, other microfabrication approaches, such as grayscale photolithography [24] and ink-jet printing [25], can be employed.

Fig. 3 plots $I_{e,\Omega,\mathrm{NORMAL}}$ as a function of h for μ-LED-coupled microlenses with the optimized θ_1 of 45° and varied d_1 ranging from 350 μm to 600 μm. As can be seen, the collimation capability of the microlens can be improved as h appropriately increases. Especially, an optimal $I_{e,\Omega,\mathrm{NORMAL}}$ of 0.54 W/sr was achieved from a microlens with $d_1 = 450\ \mu$m and $\theta_1 = 45°$ while $h = 100\ \mu$m.

D. Optimization of Reflector Structure

In this part, a reflector was further integrated on the backside of the μ-LED chip, which had been coupled with an optimized microlens. 90% reflectance was applied to simulate the high reflectivity of the surface. In the simulation, the diameter (d_2) and the inclined angle (θ_2) of the reflector varied from 300 μm to 600 μm and from 30° to 60°, respectively. Simulation result of $I_{e,\Omega,\mathrm{NORMAL}}$ in relation to d_2 and θ_2 is presented in Fig. 4, which shows great enhancement on $I_{e,\Omega,\mathrm{NORMAL}}$ compared to the device without a reflector. It can be attributed to the effective collection of the downward-emitting LED light. The maximum of $I_{e,\Omega,\mathrm{NORMAL}}$ (1.04 W/sr) appears as $d_2 = 600\ \mu$m and $\theta_2 = 45°$, which were chosen as the dimensions for the optimized reflector.

E. Performance of Optimized Structure

So far, we have investigated the structure of both microlens and reflector, and their optimized dimensions have been found.

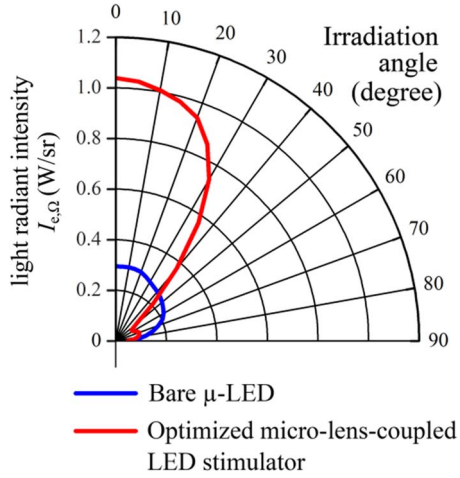

Fig. 5. Simulated candela distribution of the bare μ-LED and the optimized micro-lens-coupled LED stimulator. The light radiative flux from each side of the μ-LED was set to 1 W.

To avoid confusion, in this paper, the term"micro-lens-coupled LED stimulator" is uniquely used to describe the μ-LED chip coupled with both microlens and reflector. Fig. 5 plots the simulated polar candela distribution of the optimized micro-lens-coupled LED stimulator, as well as the distribution of the bare μ-LED for comparison. It clearly shows that the optimized micro-lens-coupled LED stimulator can effectively enhance the light irradiance at small irradiation angles (< 30°). Especially, $I_{e,\Omega,\mathrm{NORMAL}}$ increased from 0.29 W/sr to 1.04 W/sr when the light radiative flux was set to 1 W on each side of the μ-LED.

In order to mimic the application of the device in a biological environment, the penetration of light in the medium of tissue for the micro-lens-coupled LED stimulator was also simulated. At this time, the measured light radiative flux of μ-LEDs under an applied voltage of 2.9 V, which results in 2.06 mW on each side, was used to investigate the effective region in which optogenetic opsins can be stimulated. This voltage

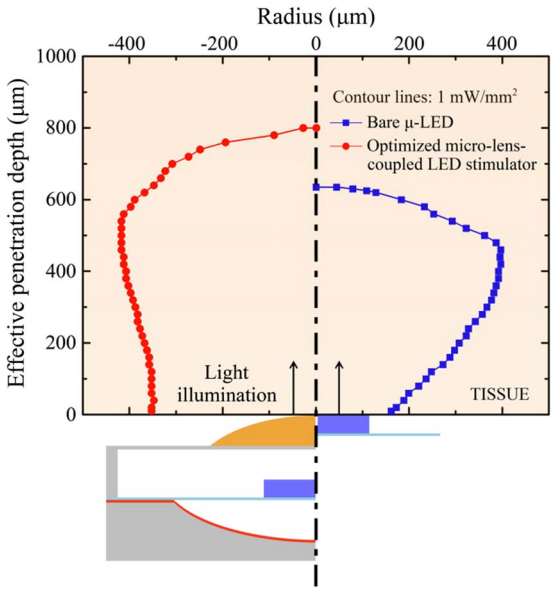

Fig. 6. Simulated contour lines at 1 mW/mm^2 in rat cortex for the optimized micro-lens-coupled LED stimulator (red) and the bare μ-LED (blue). The light radiative flux from each side of the μ-LED was set to 2.06 mW, which was measured under an applied voltage of 2.9 V.

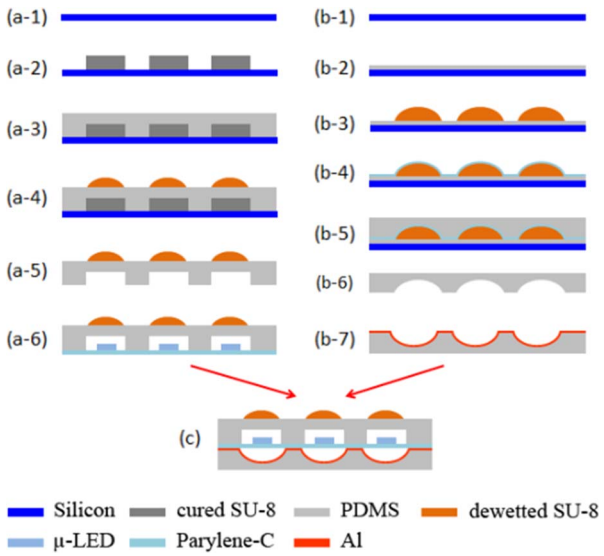

Fig. 7. Schematic illustration of fabrication and integration processes of the micro-lens-coupled LED simulator. (a) Microlens fabrication. (b) Reflector fabrication. (c) Device integration.

(2.9 V) was selected because it can provide strong illumination while avoiding overheating of the brain tissue as demonstrated previously in [26]. An absorption coefficient (μ_a) of 0.5 cm^{-1} and a reduced scattering coefficient (μ_s') of 15 cm^{-1} were employed as the transmitting property of the light in the rat cortex at a wavelength of 460 nm [27]. The contour lines at 1 mW/mm^2, which is the typical threshold of light intensity for activating excitatory opsins [19], are plotted in Fig. 6. Since the light source is typically placed in contact with the surface of the brain tissue during optogenetic experiments, a term of effective penetration depth (d_{eff}) is defined as how far the light propagates through the illuminated medium. For the lens-coupled LED stimulator, it is the distance between the target position and the summit of the microlens, rather than the μ-LED top surface. As shown in Fig. 6, the optimized micro-lens-coupled LED stimulator shows an evocable effective penetration depth of 800 μm, an increase of 26.0% compared to 635 μm for the bare μ-LED chip. The volume of stimulated tissues (with light intensity larger than 1 mW/mm^2) for the micro-lens-coupled LED stimulator and the bare μ-LED is 0.328 mm^3 and 0.193 mm^3, respectively, corresponding to an increase of 70.4%.

III. Fabrication of Device Prototypes

For the proof-of-concept, prototypes of micro-lens-coupled LED stimulators with the optimized dimensions, i.e., $d_1 = 450$ μm, $\theta_1 = 45°$, $h = 100$ μm, $d_2 = 600$ μm, and $\theta_2 = 45°$, have been fabricated. The fabrication and integration processes are schematically illustrated in Fig. 7. SU-8 pillars (MicroChem Corp.), with dimensions of 400 μm $\times$ 600 μm $\times$ 140 μm, were first patterned on silicon substrates through photolithography, followed by spin-coating a layer of 150 μm-thick PDMS mixture (Dow Corning Sylgard 184, 10 : 1 by weight). Surface plasma treatment (PX-250, March Instruments) and vapor-induced dewetting (VID) were subsequently applied to fabricate self-organized SU-8 microlenses with a diameter of 450 μm and an inclined angle of 45° at designated spots on the PDMS surface. Experimental details of the VID process for microlens fabrication have been previously reported by our group [23]. After the microlenses were formed, the PDMS cover was cut and peeled off for the preparation of assembly.

The VID process was also employed for fabricating backside reflectors, as shown in Fig. 7(b). SU-8 microlenses with a diameter of 600 μm and an inclined angle of 45° were obtained and served as the master for PDMS micromolding. A 300 nm-thick aluminum film was subsequently deposited through thermal evaporation (Edwards Auto 306 Evaporator) on the surface of the embossed PDMS to form a reflecting layer.

Surface mounted μ-LED chips (Cree TR2227TM, 220 μm $\times$ 270 μm $\times$ 50 μm) were soldered on flexible, micro-patterned circuit on a Parylene-C substrate. Prototypes of micro-lens-coupled stimulators were assembled by centrally aligning each component under a stereo microscope and then bonding with a polymer adhesive [Fig. 7(c)]. Finally, a 10-μm-thick Parylene-C deposition was performed to provide devices corrosion protection and electrical insulation. Fig. 8 presents an optical image of an integrated device, as well as the profiles of as-fabricated microlenses and reflectors that were examined by a surface profiler (NanoMap 500LS, AEP Technology). The measurement was carried out on five integrated LED stimulators and the average was taken. The microlens shows a base diameter of 458.5 ± 2.3 μm and an inclined angle of $42.7 \pm 1.1°$, while the reflector has a diameter of 606.5 ± 3.0 μm and an angle of $41.6 \pm 1.2°$.

IV. Optical Measurement

A. Measurement in Air

The optical performance of a fabricated device prototype of micro-lens-coupled LED stimulator was characterized in air

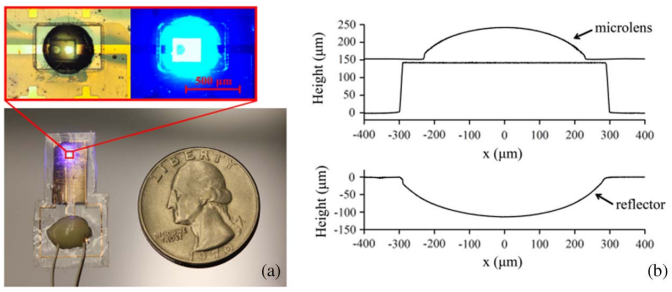

Fig. 8. (a) Optical image of an integrated micro-lens-coupled stimulator with optimized dimensions. The inset shows micrographs of the device without (left) and with (right) light illumination. (b) Profilometer measurement of the microlens and the reflector of an integrated micro-lens-coupled LED stimulator, which shows a profile of $d_1 = 461.2\ \mu$m, $\theta_1 = 42.4°$, $d_2 = 602.0\ \mu$m, and $\theta_2 = 41.5°$.

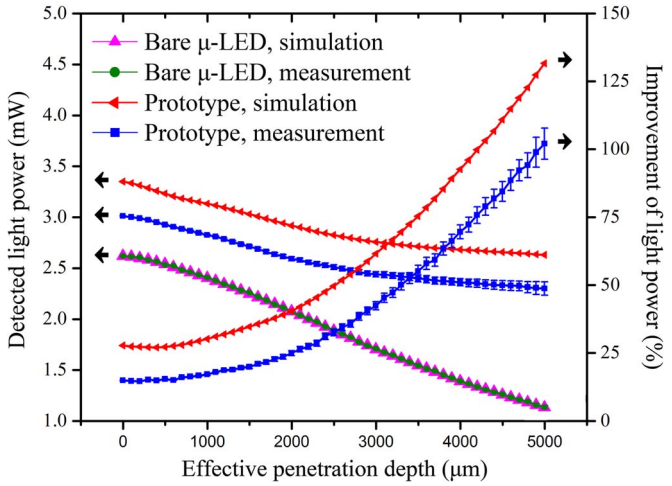

Fig. 9. Detected light power of a device prototype of the optimized micro-lens-coupled LED stimulator and the corresponding μ-LED under an applied voltage of 2.9 V, as well as the improvement of the light power for the measured prototype, as a function of the effective penetration depth. The photodetector has a sensing area of $\sim$100 mm^2. For comparison, the simulation result was also plotted.

using a photodetector (Model 815 Series, Newport, Inc), which has an approximate sensing area of 100 mm^2 to measure the incident light power. The photodetector was fixed on a 3D micropositioning stage to be able to adjust the distance between the detector and the device prototype (i.e., effective penetration depth, d_{eff}). The prototype was lit up with a fixed driving voltage of 2.9 V. The d_{eff} was gradually changed from 0 to 5 000 μm with every single step of 100 μm. Three times of measurements were carried out for the prototype before it was disassembled and the light power of the corresponding bare μ-LED was measured in the same method for another three times. The measurement result was averaged and plotted in Fig. 9. For comparison, Fig. 9 also presents the result of the simulation, in which an observation disk with a sensing area of 100 mm^2 was placed at varied depths to collect the incident light power. The applied LED source property (2.06 mW) was determined in such a way that the simulation and the measurement show an identical light power at $d_{\text{eff}} = 0$ for the bare μ-LED. The percentage of the improvement of light power for the measured prototype was calculated and also included in Fig. 9.

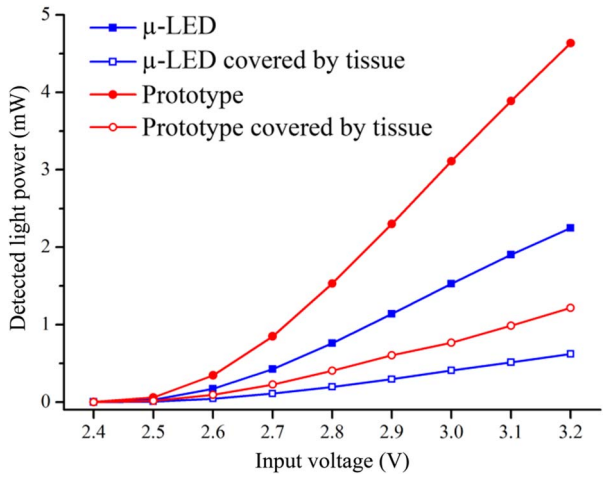

Fig. 10. Detected light power of a device prototype of the optimized micro-lens-coupled LED stimulator (red) and the corresponding bare μ-LED (blue) under different driving voltages, which was measured with (hollow) and without (solid) a $\sim$500-μm-thick rat cortical tissue slice. The photodetector has a sensing area of $\sim$100 mm^2, which was positioned at a fixed effective penetration depth of 5 000 μm.

As can be seen, the simulation and measurement results for the bare μ-LED are very consistent, as the corresponding two curves almost completely overlap. For the device prototype, the measurement result is 11% lower than the simulation on average, which is possibly due to the low reflectance of the reflector, as some wrinkles were observed on the aluminum thin film during assembly. As d_{eff} increases from 0 to 5 000 μm, the fabricated micro-lens-coupled LED stimulator achieves an improvement of light power from 15% to 102%, compared to the bare μ-LED. The improvement keeps increasing as the distance goes further, which is an evidence of the collimation effect resulted by the microlens. It implies that micro-lens-coupled LED stimulators could be more valuable in deep brain stimulation.

B. Measurement Through Tissue

In this measurement, the d_{eff} was fixed as far as 5 000 μm. An approximate 500- μm-thick rat cortical tissue slice was cut after an animal surgery and kept in saline. When applied, the tissue was taken out using a brush and placed directly on the top of the device. The light power was measured by the photodetector for one fabricated device prototype and the corresponding μ-LED, as shown in Fig. 10. An average 99% and 103% improvement was obtained with and without the 500- μm-thick rat tissue under various voltages of 2.4–3.2 V for the measured prototype, respectively. The proposed micro-lens-coupled LED stimulator demonstrates a remarkable potential to enable optical neural stimulation with a lower driving voltage on μ-LEDs, and thus prevent excessive heat production and reduce the risk of tissue damage.

C. Soaking Test

Soaking test was initiated by immersing two device prototypes in saline (0.9 wt% sodium chloride) on a hot plate set at

40 °C for seven days, to evaluate the reliability of the lens-coupled LEDs. One device (A) was kept on by applying a continuing pulsed signal with a voltage of 2.7 V and a duty cycle of 50%, while the other one (B) was disconnected. After seven days, device A shows a decrease of 11.8% in the light power at $d_{\text{eff}} = 0$, while device B did not show any deterioration of optical throughput. Soaking test study is ongoing for the statistical analysis of device's long-term reliability and the in-depth understanding of potential failure mechanisms.

V. Conclusion

A micro-lens-coupled LED neural stimulator, consisting of a μ-LED, a frontside microlens, and a backside reflector was proposed as the light source for optical neural stimulation. An optimization of the device structure was carried out in order to attain optimal collimation and penetration capabilities of light. The simulation shows that the optimized micro-lens-coupled LED stimulator is able to activate excitatory opsins with 26.0% increase in penetration depth and 70.4% increase in the volume of stimulated tissue. The optimized microlenses and reflectors were fabricated through vapor-induced dewetting followed by integration with surface-mounted μ-LED chips to obtain device prototypes. The light power was measured by a photodetector and the fabricated device prototype shows an improvement of 15% to 102% as the effective penetration depth increased from 0 to 5 000 μm, compared to the bare μ-LED. While applying a 500-μm-thick rat cortical tissue slice, an average 99% light power enhancement at $d_{\text{eff}} = 5,000$ μm was achieved by the micro-lens-coupled LED stimulator under various voltages.

The proposed micro-lens-coupled LED stimulator demonstrates a remarkable potential to enable optical neural stimulation with increased volumetric recruitment of excitable tissues, which is critical for inducing behavioral changes in large animals and non-human primates [13], [28]. In addition, reducing the input voltage of μ-LEDs potentially prevents excessive heat production, thereby reducing the risk of thermally-induced interferences and tissue damage. *In-vitro* and *in-vivo* testing will be carried out in the future study to validate the functionality of the fabricated devices in optical neural stimulation.

References

[1] G. Nagel *et al.*, "Channelrhodopsin-2, a directly light-gated cation-selective membrane channel," *Proc. Nat. Acad. Sci. USA*, vol. 100, no. 24, pp. 13940–13945, Nov. 2003.

[2] B. Schobert and J. K. Lanyi, "Halorhodopsin is a light-driven chloride pump," *J. Biol. Chem.*, vol. 257, no. 17, pp. 306–313, 1982.

[3] B. Y. Chow *et al.*, "High-performance genetically targetable optical neural silencing by light-driven proton pumps," *Nature*, vol. 463, no. 7277, pp. 98–102, Jan. 2010.

[4] A. Stroh and I. Diester, "Optogenetics: A new method for the causal analysis of neuronal networks in vivo," *Neuroforum*, vol. 18, no. 4, pp. 280–289, Nov. 2012.

[5] M. Banghart, K. Borges, E. Isacoff, D. Trauner, and R. H. Kramer, "Light-activated ion channels for remote control of neuronal firing," *Nat. Neurosci.*, vol. 7, no. 12, pp. 1381–1386, Dec. 2004.

[6] K. Deisseroth, "Optogenetics," *Nature Methods*, vol. 8, no. 1, pp. 26–29, Jan. 2011.

[7] L. Buchen, "Neuroscience: Illuminating the brain," *Nature*, vol. 465, no. 7294, pp. 26–28, May 2010.

[8] S. Butovas and C. Schwarz, "Spatiotemporal effects of microstimulation in rat neocortex: A parametric study using multielectrode recordings," *J. Neurophys.*, vol. 90, no. 5, pp. 3024–3039, Nov. 2003.

[9] E. S. Boyden, F. Zhang, E. Bamberg, G. Nagel, and K. Deisseroth, "Millisecond-timescale, genetically targeted optical control of neural activity," *Nature Neurosci.*, vol. 8, no. 9, pp. 1263–1268, Sep. 2005.

[10] F. Zhang *et al.*, "Optogenetic interrogation of neural circuits: Technology for probing mammalian brain structures," *Nature Protoc.*, vol. 5, no. 3, pp. 439–456, 2010.

[11] V. Gradinaru *et al.*, "Targeting and readout strategies for fast optical neural control in vitro and in vivo," *J. Neurosci.*, vol. 27, no. 52, pp. 14231–14238, Dec. 2007.

[12] A. M. Aravanis *et al.*, "An optical neural interface: In vivo control of rodent motor cortex with integrated fiberoptic and optogenetic technology," *J. Neural Eng.*, vol. 4, no. 3, pp. S143–S156, Sep. 2007.

[13] X. Han *et al.*,"Millisecond-timescale optical control of neural dynamics in the nonhuman primate brain," *Neuron*, vol. 62, no. 2, pp. 191–198, Apr. 2009.

[14] N. McAlinden *et al.*, "Thermal and optical characterization of micro-LED probes for in vivo optogenetic neural stimulation," *Opt. Lett.*, vol. 38, no. 6, pp. 992–994, Mar. 2013.

[15] C. T. Wentz, J. G. Bernstein, P. Monahan, A. Guerra, A. Rodriguez, and E. S. Boyden, "A wirelessly powered and controlled device for optical neural control of freely-behaving animals," *J. Neural Eng.*, vol. 8, no. 4, p. 10, Aug. 2011.

[16] K. Y. Kwon, H. M. Lee, M. Ghovanloo, A. Weber, and W. Li, "A wireless slanted optrode array with integrated micro LEDs for optogenetics," in *Proc. IEEE 27th Int. Conf. Micro Electro Mechanical Systems*, San Francisco, CA, USA, 2014, pp. 813–816.

[17] N. Grossman *et al.*, "Multi-site optical excitation using ChR2 and micro-LED array," *J. Neural Eng.*, vol. 7, no. 1, p. 13, Feb. 2010.

[18] B. McGovern *et al.*, "A new individually addressable micro-LED array for photogenetic neural stimulation," *IEEE Trans. Biomed. Circuits Syst.*, vol. 4, no. 6, pp. 469–476, Dec. 2010.

[19] E. Stark, T. Koos, and G. Buzsaki, "Diode probes for spatiotemporal optical control of multiple neurons in freely moving animals," *J. Neurophysiol.*, vol. 108, no. 1, pp. 349–363, Jul. 2012.

[20] K. Y. Kwon, A. Khomenko, M. Haq, and W. Li, "Integrated slanted microneedle-LED array for optogenetics," in *Proc. 35th Int. Conf. IEEE Engineering in Medicine And Biology Soc.*, Oaska, Japan, Jul. 2013, pp. 249–252.

[21] Y. Sun and S. R. Forrest, "Enhanced light out-coupling of organic light-emitting devices using embedded low-index grids," *Nature Photon.*, vol. 2, no. 8, pp. 483–487, Aug. 2008.

[22] X. Bi, B. Fan, and W. Li, "Micro-lens-coupled LED neural stimulator for optogenetics," in *Proc. IEEE Int. Conf. Biomedical Circuits and Systems Conf.*, Atlanta, GA, USA, Oct. 2015, pp. 1–4.

[23] X. Bi and W. Li, "Fabrication of flexible microlens arrays through vapor-induced dewetting on selectively plasma-treated surfaces," *J. Mater. Chem. C*, vol. 3, no. 22, pp. 5825–5834, 2015.

[24] K. Totsu, K. Fujishiro, S. Tanaka, and M. Esashi, "Fabrication of three-dimensional microstructure using maskless gray-scale lithography," *Sens. Actuators A, Phys.*, vol. 130, pp. 387–392, Aug. 2006.

[25] J. Y. Kim, K. Pfeiffer, A. Voigt, G. Gruetzner, and J. Brugger, "Directly fabricated multi-scale microlens arrays on a hydrophobic flat surface by a simple ink-jet printing technique," *J. Mater. Chem.*, vol. 22, no. 7, pp. 3053–3058, 2012.

[26] K. Y. Kwon, B. Sirowatka, A. Weber, and W. Li, "Opto-μECoG array: A hybrid neural interface with transparent μECoG electrode array and integrated LEDs for optogenetics," *IEEE Trans. Biomed. Circuits Syst.*, vol. 7, no. 5, pp. 593–600, 2013.

[27] B. Gysbrechts *et al.*, "Light distribution and thermal effects in the rat brain under optogenetic stimulation," *J. Biophotonics*, pp. 1–10, 2015.

[28] I. Diester *et al.*, "An optogenetic toolbox designed for primates," *Nature Neurosci.*, vol. 14, no. 3, pp. 387–397, 2011.

Xiaopeng Bi received the M.S. degree in electrical engineering from Michigan State University (MSU), East Lansing, MI, USA, in 2013.

Currently, he is working toward the Ph.D. degree in the Microtechnology Laboratory in the Department of Electrical and Computer Engineering at MSU. His research is mainly focuses on bio-MEMS materials, devices, and systems.

Tian Xie is working toward the B.S. degree in electrical and computer engineering at Michigan State University, East Lansing, MI, USA.

He is an undergraduate Research Assistant in the Microtechnology Laboratory. His research focuses on the simulation and fabrication of optogenetic LED stimulators.

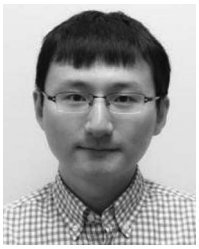

Bin Fan received the B.S. and M.S. degrees in electrical and computer engineering from Nankai University, Tianjin, China, in 2008 and 2011, respectively.

Currently, he is working toward the Ph.D. degree in electrical and computer engineering at Michigan State University, East Lansing, MI, USA. His research interests include flexible/wearable diamond sensors for chemical sensing and neural interfaces, sensor interfacing circuit, microwave resonators, antenna and circuits, and superconducting Josephson junction arrays for microwave applications.

Wasif Khan received the B.S. degree from the Military Institute of Science and Technology, Dhaka, Bangladesh, in 2010, and the M.S. degree from Michigan State University (MSU), East Lansing, MI, USA, in 2016, both in electrical engineering.

Currently, he is working toward the Ph.D. degree in electrical engineering at MSU. His research interests include neural interfaces, optical stimulators for optogenetics, microsystems integration, and packaging technologies.

Yue Guo received the B.S. degree in electrical engineering from Michigan State University (MSU), East Lansing, MI, USA.

Since 2013, he has been an undergraduate Researcher Assistant in the Microtechnology Laboratory at MSU and became a Ph.D. student in the same group in 2016. His research includes the microfabrication of intraocular monitoring sensors (IOP sensors), ECOG neural sensors, and boron-doped diamond neural sensors.

Wen Li (S'03–M'09–SM'14) received the M.S. and Ph.D. degrees in electrical engineering from the California Institute of Technology, Pasadena, CA, USA, in 2004 and 2008. respectively.

Currently, she is an Associate Professor of Electrical and Computer Engineering at Michigan State University, East Lansing, MI, USA. Her research focuses on MEMS/NEMS, neuroprosthetic devices, micro/nano sensors and actuators, nanoelectronics, as well as microsystem integration and packaging technologies.